SF2A 2007
J. Bouvier, A. Chalabaev, C. Charbonnel (eds)

THE VISIBILITY OF LYMAN-ALPHA EMISSION IN STARBURST GALAXIES: THE ROLE OF THE DUST

H. Atek[1] and D. Kunth[1]

Abstract. We present the results of local straburst galaxies imaging with the HST/ACS and NTT/NOT observations. HST/ACS narrow bands imaging allows us, using an elaborated SED modeling method with Starburst 99, to correctly subtract the extrapolated continuum from F140LP to F122M to get Lyα line image. Hα and Hβ observations have been carried out on the ground based facilities, the ESO New Technology Telescope (NTT) and the Nordic Optical Telescope (NOT). We have generated extinction maps using the Balmer decrement Hα/Hβ to investigate the dust in the gas phase. With dust maps and continuum-subtracted Lyα images, we have undertaken a correlation studies between all the relevant parameters, that could explain the escape mechanism of Lyα photons, in each galaxy at a very small scale. We found that, for the six galaxies in our sample, the bulk of Lyα is seen in a diffuse and low surface brightness componenent, hence highlighting the effect of resonant scattering in the neutral gas. The escape fraction of Lyα photons is still very small and never exceed 15%. Not only the Hα and UV continuum morphology is not correlated with the Lyα one, but even the dust appears to not really explain in all cases the visibility of the Lyα line. The dust is the main regulator of the Lyα escape in a static and homogeneous medium. Otherwise, the kinematics of the neutral ISM and its porosity and geometry may play a more significant role.

1 Introduction

For almost four decades the cosmological significance of the Lyα emission line has been realised (Partridge & Peebles 1967). Young galaxies, dominated by massive hot stars are expected to produce strong Lyα emission lines, with equivalent width around 100 Å(Charlot & Fall 1993; Schaerer 2003). It has been conjectured that primeval galaxies at their early stage would be nearly dust-free and hence easily detectable thanks to their Lyα emission.

However the first generation of surveys failed to uncover the predicted population of Lyα emitting galaxies (Pritchet 1994) as the initial predictions had been too optimistic. nearby, low-metallicity starburst galaxies should in principle ressemble those at high-redshift. Early ultraviolet observations of nearby starburst galaxies have revealed, in most cases, much weaker Lyα emission than predicted by simple models of galaxy formation. In some other objects Lyα was non-existent or appeared as a braod absorption profile (Meier & Terlevich 1981, Hartmann et al. 1984, Hartmann et al. 1988, Terlevich et al. 1993). HST observations unveiled much more the complexity of Lyα escape. Kunth et al. (1994) found no trace of emission, but a damped absorption in IZw 18, the most metal poor object known. This correlation was not expected, since the dust content generally follows the metallicty. On the other hand, Lequeux et al. (1995) detected a prominent emission line in Haro 2, another gas-rich galaxy but with much higher oxygen abundance than IZw 18. GHRS spectra showed a P Cygny profile with a strong, blueshifted absorption. Interstellar absorption lines were blueshifted by $\sim$ 200 km s^{-1} with respect to the ionized regions. It became clear, from these early studies, that, some other processes must be at work in these regions. The Lyα intensity is weakened by internal dust extinction, especially in the far UV, attenuating both line and continuum photons. In addition, resonant scattering makes Lyα photons path much longer hence increasing the probability of dust absorption. the geometry and the porosity of the ISM may play also an important role (Giavalisco et al. 1996).

High-z Lyα emitters are now routinely detected since the main breakthrough of Cowie & Hu (1998). Lyα line is now recognized as the best tracer of galaxy formation in the high-z Universe. It serves the detection of

[1] Institut d'Astrophysique de Paris (IAP), 98bis, boulevard Arago, 75014 Paris, France

© Société Francaise d'Astronomie et d'Astrophysique (SF2A) 2007

high-z candidates by the Lyman-break technique as well as the detection or the confirmation of LBGs candidates by using the emission itself. It also serves cosmological studies, from the star formation rates (SFR) (Fujita et al. 2003, Gronwall et al. 2007) to ionization fraction the IGM (Kashikawa et al. 2006, Dijkstra et al. 2007). However, without a full understanding of the different processes that may be at work, Lyα only can not be used to estimate cosmological quantities such as star formation rates or clustering factors. These considerations led us to start a pilot program to image local Lyα emitters using space and ground-based facilities (Kunth et al, 1998).

We present here, the result of our HST/ACS Lyα imaging of six local straburst galaxies, combined with Hα and Hβ images in order to investigate the role of the dust in the Lyα escape mechanism. We particulary focus on Haro 11, one of our six nearby galaxies and present global properties of the sample.

2 Haro 11

This galaxy is a well known Lyα emitter (Kunth et al. 1998) and the only known nearby emitter of Lyman Continuum (Bergvall et al. 2006). It has been studied in more details in Hayes et al. (2007a). The Hα image in Fig.1 (first image) shows a complex morphology with three main star-forming condensations (Kunth et al. 2003). The continuum subtracted Lyα image (second image) does not follow this morphology, showing Lyα in emission in only knot C, whereas it is seen in absorption in knot A and B. The emission exhibits two different conponents consisting in a central bright knot and a low surface brightness diffuse emission. It seems that, examining the extinction map (right-most frame), the latter component is not quite regulated by the dust amount. Moreover, the bright Lyα emission in knot C, corresponds to a high extinction region.

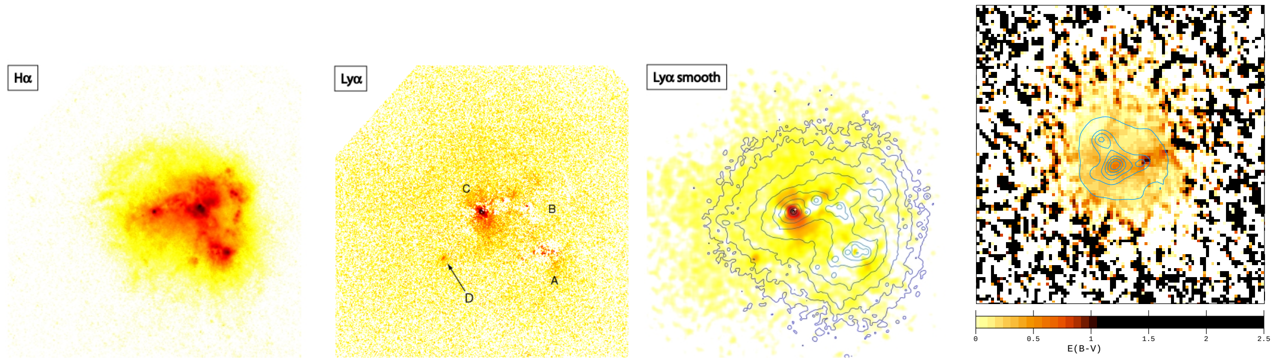

Fig. 1. HST imaging of Haro 11. The FOV is 20 × 20". Inverted scale is used showing the emission in black and absorption in white. The first image represents Hα online flux and the second is the Lyα continuum-subtracted image. The last image shows a smoothed Lyα image overlayed by FUV (1500 Å) contours. Among the three condensations observed in the FUV, only one shows Lyα in emission. The absence of correlation between resonant (Lyα) and non-resonanat (FUV continuum and Hα) radiation is striking. The right-most frame shows an E(B-V) map overlayed by Hα contours at the NTT resolution. The dusty regions are in black and dust free ones in white.

The first plot in figure 2 presents the correlation between the Lyα emission and the extinction determined from the Balmer decrement tracing the dust in the gas phase ($E_{B-V,\mathrm{gas}}$). The color-code represents different regions of interest consisting in circular apretures centered on the three main knots of the galaxy, and are marked on the Lyα image. We can see a diffuse emission component extending up to $E_{B-V} \sim 2$. The knot C shows a brighter spread-out emission with a mean extinction of 0.48, while the absorption is essentialy localised around knot A and B.

The presence of two emission components is indicative of two different physical processes implied in the escape of Lyα photons. The diffuse component shows the resonant decoupling of Lyα photons which have to resonantly scatter on hydrogen atoms until they escape far away from there production sites and, thus, experiencing a large range of extinction. On the other hand, the emission from knot C is less spread-out and represents photons escaping directly from this small region that corresponds to a mean extinction $E_{B-V} \sim 0.48$. We observe a first component at a low and roughly constent Lyα flux ($\lesssim 10^{-14}$ erg s^{-1} cm^{-2}), independant of Hα emission and where Lyα /Hα may exceed the level predicted by the Case B in recombination theory (represented by a solid line in the figure). Thanks to their resonant scattering, Lyα photons reach regions where non-resonant photons, such as Hα , are absent, making the Lyα /Hα ratio higher than the Case B level. The second component at higher Lyα and Hα fluxes ($f_{\mathrm{Ly}\alpha} \geq 10^{-14}$ erg s^{-1} cm^{-2})is always below the predicted recombination value. These pixels represent regions where Lyα photons escape directly from their production site where Hα is also produced.

That we see Lyα in emission from knot C with $E_{B-V} \sim 0.48$ whereas absorption is seen in knots A and B with $E_{B-V} \sim 0.2$ and 0.41 respectively, is surprising. It seems that Lyα photons manage to escape from regions with higher extinction than that required for a pure absorption. This indicates that the dust content might not be the only or the dominant parameter in the escape process of Lyα photons. A great covering of static HI column density in knot A and an expanding neutral ISM and/or ionised HII holes in knot C may lead to this observation.

Looking at Lyα equivalent width (Fig. 2, second plot), we observe a decline of the pure emission from knot C (in red) with the dust content. It means that the Lyα continuum is higher in the region where we see a strong Lyα flux, making $EW_{\mathrm{Ly}\alpha}$ smaller. This suggests that a hard FUV radiation could creates ionised holes through which Lyα photons may escape, in a inhomogeneous ditribution of HI and dust. In this case of multi-phase ISM, it has been shown (Neufeld, 1991; Hansen & Oh, 2006) that, thanks to their scattering on the dusty HI clumps, Lyα might escape in an easier way than non-resonant photons. We also observe that the diffuse emission (in cyan) corresponds to the highest equivalent width observed ($EW_{\mathrm{Ly}\alpha}$ up to 200 $\mathring{A}$), since it represents photons that have scattered far away from their production sites and escape where the Lyα continuum is lower. This decline in the emission is, again, symptomatic of the resonant nature of Lyα photons. Indeed, when we plot the equivalent width of Hα against the extinction, we do not see any correlation, as we expect for non-resonant lines, since the online and the continuum photons are regulated by the same physical processes according to the dust content. The fourth plot in Fig. 2 shows how the Lyα /Hα ratio evolves according to the amount of dust. In a classical view, considering only the selective extinction at the two wavelengths, and a case B intrinsic ratio of 8.7, we expect to have an exponential decline represented by the dark curve. The resonant nature of the Lyα photons leads to a different result. We observe a high dispersion for the halo component and an emission from knot C above the predicted level at higher extinction, which supports the view of a scattering in inhomogeneous ionised ISM enhancing preferentially the ecape of Lyα photons.

3 The role of the dust in the escape of Lyα photons

Target	$f_{\mathrm{Ly}\alpha}$ [erg s^{-1} cm^{-2}]	$f_{\mathrm{H}\alpha}$ [erg s^{-1} cm^{-2}]	$f_{\mathrm{H}\beta}$ [erg s^{-1} cm^{-2}]	Lyα/Hα	Hα /Hβ	EW(Lyα) [Å]	EW(Hα) [Å]
Haro 11	1.3e-12	2.3e-12	5.24e-13	0.58	4.18	22.8	524.4
ESO 338-IG04	1.4e-12	1.8e-12	5.2e-13	0.74	3.55	13.5	501.7
SBS 0335-052	-3.5e-13	2.8e-13	6.4e-14	-1.22	4.40	-29.3	858.2
NGC 6090	4.4e-13	1.1e-12	1.7e-13	0.38	6.66	62.6	196.6
IRAS 08+65	1.6e-12	7e-13	1.9e-13	2.34	3.75	45.3	139.5
Tololo 65	3.7e-14	1.7e-13	4e-14	0.24	3.87	7.58	1182.7

Table 1. Integrated fluxes and equivalent widths for the six galaxies of the sample. The integration aperture is defined by masking regions below a certain threshold based upon Hβ flux ($f_{\mathrm{H}\beta} \geq 2 \times 10^{-17}$ erg s^{-1} cm^{-2}, except for Tol 65 where $f_{\mathrm{H}\beta} \geq 0.5 \times 10^{-17}$ erg s^{-1} cm^{-2}). Thus, the aperture size vary from object to other. The quantities are corrected for galactic extinction (Schlegel et al, 1998) but not for internal reddening.

We show in Table 3 the photometric properties of our sample, integrated in an aperture defined by a mask based upon a Hβ flux threshold above the sky level, in order to get the extended emission of the Balmer lines and the Lyα diffuse emission. As mentioned before, all the quantities presented have been corrected for galactic

Table 2. The role of the dust in the Lyα escape. First column represents the escape fraction of Lyα . It is determined using Hα emission and the theoritical ratio predicted by the recombination theory, compared with the observed Lyα flux. It shows how much Lyα flux escaped from the galaxy. Second column is the fraction of the diffuse component. The average extinction in each galaxy is given in the last column.

Target	f_{esc} (%)	$f_{diffuse}$ (%)	E(B-V)
Haro 11	3.8	74	0.23
ESO 338-IG04	5.3	40	0.20
SBS 0335-052	0	100	0.49
NGC 6090	0.6	44	0.8
IRAS 08+65	13.2	69	0.29
Tololo 65	1.5	~ 100	0.25

extinction using Schlegel et al. (1998) method. The integration of the Lyα flux whithin the mask aperture results in five candidates of our sample being emitters and only one net absorber (SBS 0335). Defining this galaxy as a net absorber means that the sum of the flux overall the galaxy gives a negative result, however we do see emission in some regions. Though, the flux and the measurements derived from are very sensitive to the aperture size. We can expect that we are losing a part of the weak diffuse Lyα emission and the most extended Hα or Hβ emission, which could be achieved by deeper observations. Thus, measurements such as the escape fraction of Lyα may change according to the mask size since Lyα can scatter further from the production sites than Balmer or continuum photons.

The Lyα/Hα ratio ranges from -1.22 to 2.34, showing Lyα emission much weaker for all the sample than predicted by recombination theory. Previous observations (Terlevich et al., 1993; Giavalisco et al, 1996) yields the same conclusions. The dust is just the final stage of the processus responsible for the obscuration of Lyα photons, after the resonant scattering in an homogeneous medium that increase their mean path, which makes the recombination ratio not only regulated by the dust (as seen from the Hα/Hβ ratio that traces the nebular dust). Setting the Lyα equivalent width against the different parameters of Table 3 ends up with no clear trends. However, it is interesting to note the anticorrelation that we can see in Figure 2 between $EW_{\mathrm{Ly}\alpha}$ and $EW_{\mathrm{H}\alpha}$. The former is much more sensitive to the dust amount because of the different behaviour, with respect to the dust, between the Lyα online photons and the Lyα continuum and Balmer photons. Therefore, this relation express simply the role of the resonant scattering more than the dust itself. In the same way, plotting the Lyα equivalent width against E(B-V) allows us to probe the difference in extinction between resonant and non-resonant radiations, knowing that $EW_{\mathrm{Ly}\alpha}$ is not affected by the selective extinction. We see, indeed, in Figure 2, a rather scattered data points and no well-observed correlation. since we are dealing with resonant radiation on one hand, and are investigating only one line-of-sight on the other hand, we can expect that the geometry and the distribution of the dust layers around the emitting regions may play an important role in the observed scatter of $EW_{\mathrm{Ly}\alpha}$ according to the extinction. This clearly points out again that the dust is not the only or the main responsible of the obscuration of Lyα photons.

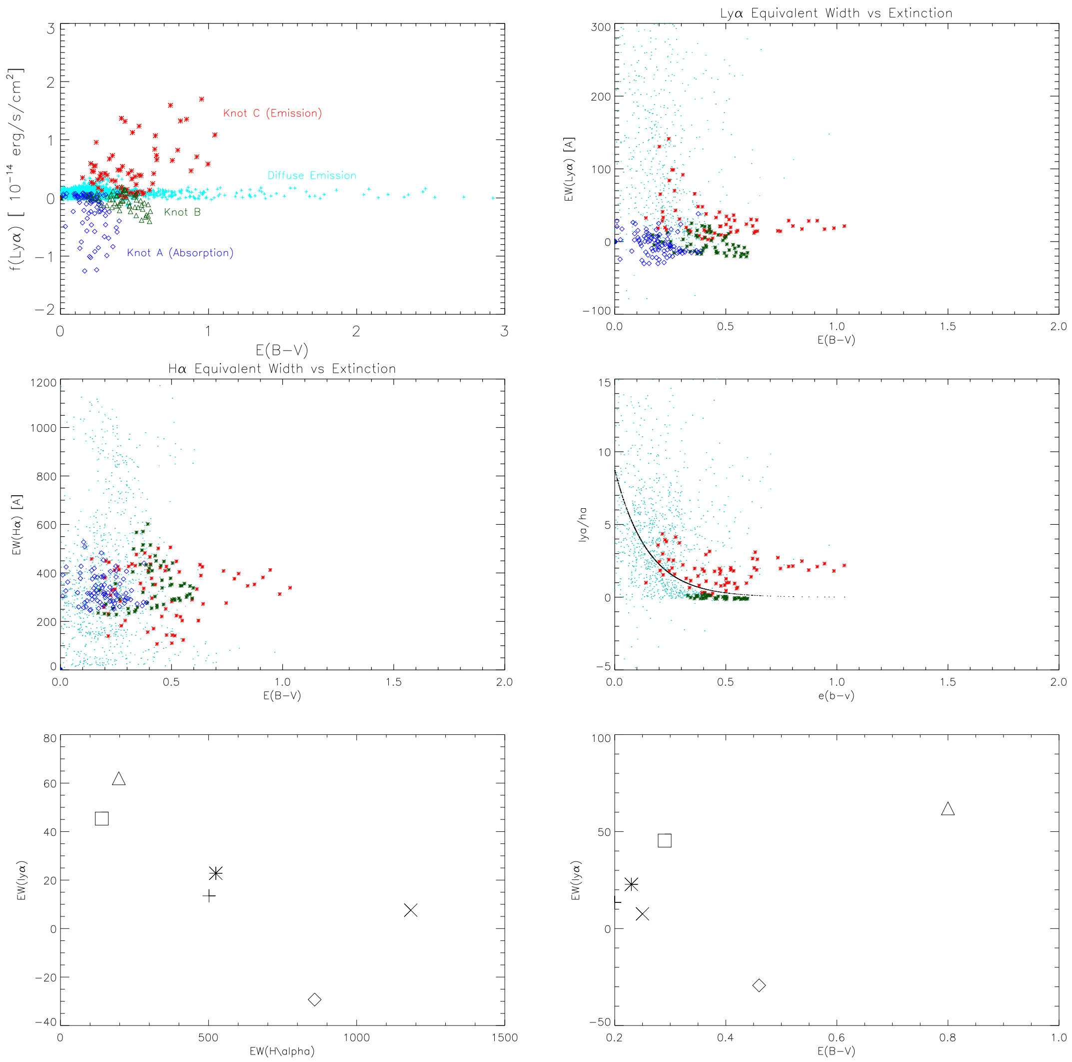

Fig. 2. *The first four plots* in this figure represent the small scale Lya correlations in the galaxy Haro 11. The first plot shows the variations of Lyα flux in function of the dust content ($E_{B-V,\mathrm{gas}}$). The different regions of interest are plotted with different colors and marked on the figure. Th eprominent componenet is the diffuse emission in cyan. The same color-code is applied for the three ramainig plots. Second and third plot present the $EW_{\mathrm{Ly}\alpha}$ and $EW_{\mathrm{H}\alpha}$ respectively against E(B-V). The evolution of tha ratio Lyα/Hα with the dust is given in the fourth plot. The black curve represents the dereddened theoritical Lyα/Hα ratio, i.e. for a given E(B-V) the expected Lyα/Hα ratio assuming only the selective extinction. The last and lower plot represents in log scale (hence the absorption is not plotted) Lyα against Hα flux. The two black lines show the predicted vlaues by the recombination theory without extinction correction. *The last two plots* represents global correlations between integrated quantities in each galaxy. Haro 11: asterisk, ESO 338: plus, SBS 0335: diamond, NGC6090: triangle, IRAS 08: square, Tol 65: cross.

4 Conclusion

Using ESO/NTT and NOT observations,we have produced extinction maps of six nearby starburst galaxies. Combined with HST/ACS observations, we have investigated the spatial variations of the Lyα emission ragarding the dust content, at a small scale. We have found a variety of Lyα morphologies, from emission to pure absorption. Lyα emission appers to vary at a very small scales where we found blended emission and absorption.

An ubiquitous diffuse Lyα emission is found in all the galaxies surrounding the emission regions and acounting for the mojotity of the total emission. We show through this emission the importance of resonant scattering in neural gas, that makes Lyα photons escape far away from their production sites. We observed in many cases, that the dust is not always the dominant parameter in the Lyα escape. Indeed, no clear correlation has been found between the escape fraction, or the $EW_{\mathrm{Ly}\alpha}$ and the dust in the gas probed by E(B-V). Moreover,we found in Haro 11, Lyα emission that emerges from regions dustier than those wher Lyα is seen in absorption. The ISM kinematics may play a more significant role in thses media making Lyα escape easier regardless of the dust content, in addition to the geomrtry and the porosity whih may work in the same way.

However our sample contains only six galaxies, and is therefore not statistically significant,we stress, knowing the complexity of tha radiative transfer of Lyα photons, that the cosmological quantities, such as SFR, derived using Lyα only, should be considered with caution.

We want to thank all collaborators We are working with. In particular, many thanks go to Daniel Schaerer and Anne Verhamme, Matthew Hayes and Göran Östlin, J. Miguel Mas-Hesse and Claus Leitherer.

References

Atek, H., Kunth, D., Hayes, M. et al. 2007, A&A, *submitted.*

Bergvall, N., Zackrisson, E., Andersson, B.-G. et al. 2006, A&A, 448, 513

Charlot, S., & Fall, S. M. 1993, ApJ, 415, 580

Cowie, L. L. & Hu, E. M. 1998, AJ, 115, 1319

Dijkstra, M., Wyithe, S., & Haiman, Z. 2007, MNRAS, 379, 253

Fujita, S. S., et al. 2003, AJ, 125, 13

Giavalisco, M., Koratkar, A., & Calzetti, D. 1996, ApJ, 466, 831

Gronwall, C., Ciardullo, R., Hickey, T. et al. 2007, ArXiv e-prints, 705

Hansen, M. & Oh, S. P. 2006, MNRAS, 367, 979

Hartmann, L. W., Huchra, J. P. & Geller M.J. 1984, ApJ, 287, 487

Hartmann, L. W., Huchra, J. P., Geller M.J. et al. 1988, ApJ, 326, 101

Hayes, M., Östlin, G., Mas-Hesse et al. 2005, A&A, 438, 71

Hayes, M.,Östlin, G., Atek et al. 2007, ApJ, *submitted.*

Kashikawa, N., Shimasaku, K., Malkan, M. A. et al. 2006, ApJ, 648, 7

Kunth, D., Lequeux, J., Sargent, W. L. W. et al. 1994, A&A, 282, 709

Kunth, D., Mas-Hesse, J. M., Terlevich, E. et al. 1998, A&A, 334, 11

Kunth, D., Leitherer, C., Mas-Hesse, J. M. et al. 2003, ApJ, 597, 263

Lequeux, J., Kunth, D., Mas-Hesse, J. M. et al 1995, A&A, 301, 18

Mas-Hesse, J. M., Kunth, D., Tenorio-Tagle, G., Leitherer, C. et al. 2003, ApJ, 598, 858

Meier, D. L. & Terlevich R. 1981, ApJ, 246, L109

Neufeld, D. A. 1991, ApJL, 370, L85

Partridge, R. B., & Peebles, P. J. E. 1967, ApJ, 147, 868

Pritchet, C. J. 1994, PASP, 106, 1052

Schaerer, D. 2003, A&A, 397, 527

Schlegel, D. J., Finkbeiner, D. P., & Davis, M. 1998, ApJ, 500, 525

Terlevich, E., Diaz, A. I., Terlevich, R. et al. 1993, MNRAS, 260, 3

Thuan, T. X., & Izotov, Y. I. 1997, ApJ, 489, 623

Verhamme, A., Schaerer, D., & Maselli, A. 2006, A&A, 460, 397